

between D1 and CP43 or D2 and CP47 or close to the position of Q_C. All of the Xe sites were found at >17 Å distance to the redox active cofactors involved in charge separation and transmembrane electron transfer.

This suggests that the hydrophobic patches in the interior of PSII, formed partly by lipids, allow diffusion of oxygen formed at the luminal side through PSII to the cytoplasmic side. As these patches have a higher affinity to oxygen compared to the other regions of the PSII complex their arrangement apparently provides means to keep oxygen away from the RC region and to prevent oxidative damage to the highly reactive pigments that are involved in charge separation and ET.

This proposed function of the hydrophobic patches within PSII could be an additional reason (apart from allowing fast disassembly/assembly and from fine tuning binding and properties of other cofactors) for the high lipid content of PSII, when compared to PSI, the *cyt b₆f* complex and other protein complexes, as PSII is both, the source of oxygen, and the protein complex most susceptible to oxidative damage in the thylakoids.

3.2.2 Plastoquinones

Among the cofactors found in PSII, there are two plastoquinones with 9 isoprenoid units in the tail (PQ9) that are part of the ETC and located in Q_A- and Q_B-sites. The primary electron donor Chl_{D1} donates the released electron through the primary electron acceptor pheophytin (Phe_{D2}) to PQ in Q_A-site that serves as an electron transmitter and sends the electron to the terminal electron acceptor PQ in the Q_B-site (see also section 1.2). This plastoquinone Q_B acts as substrate because it is doubly reduced by two electron passes, and, after double protonation, leaves PSII as plastoquinol, PQH₂, thereby taking electrons away from PSII and preventing back-reactions.

3.2.2.1 Plastoquinone Q_A

Q_A is immobile, because its head group as well as the isoprenoid tail are fixed by amino acids from subunit D2. The Q_A-binding site is formed mainly by hydrophobic residues Ile213, His214, Thr217, Val218, Thr221, Tyr244, Met246, Ala249, Asn250, Trp253, Ala260, Phe261 and Leu267 (all conserved). The head group of Q_A partially stacks with the indol ring

of Trp253, and two short hydrogen bonds are formed between conserved amino acids from subunit D2 and the quinone oxygens: Phe261N \cdots O1-Q_A (2.83 Å) and His214ND \cdots O2-Q_A (2.61 Å) (Fig. 37A).

The isoprenoid tail of Q_A is bent $\sim 90^\circ$ between isoprenoid units 4 and 5, and inserted between TMHs of the small subunits PsbL, PsbT and TMH **d** of D2, and TMH **a** of D1. The double bond of the terminal isoprenoid unit is sandwiched between the π -electron clouds of the phenyl rings of conserved D1-Phe52 and PsbT-Phe10 (edge to edge distances 3.75 Å) (Fig. 37B), providing additional fixation of the Q_A molecule. Its isoprenoid tail is at van der Waals contact to the chlorin ring and phytol chain of the accessory chlorophyll Chl_{D1} and stabilizes this primary electron donor in its position (Fig 37C).

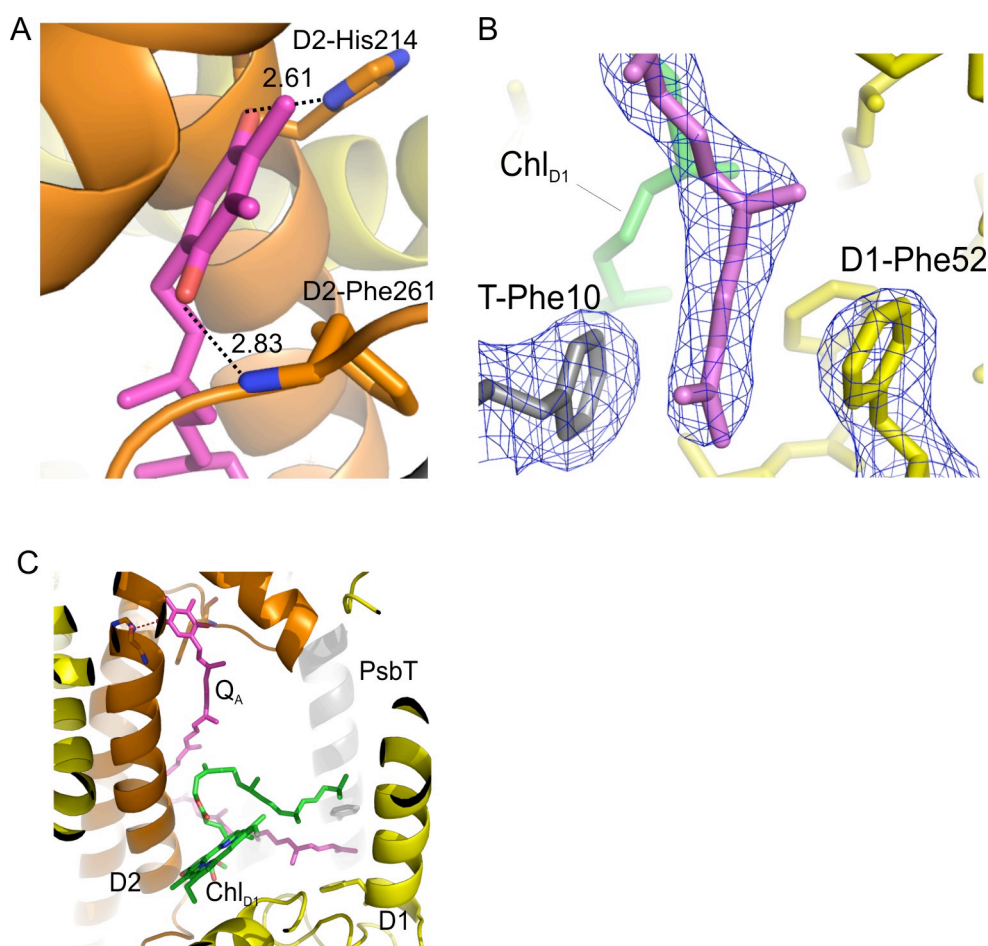


Figure 37. Plastoquinone Q_A interactions. A) Hydrogen bonds between quinone head group (magenta) and protein (D2 in orange and D1 in yellow). Distances are in Å. B) The terminus of the isoprenoid chain of Q_A (magenta) is sandwiched between phenyl rings D1-Phe52 (yellow) and PsbT-Phe10 (grey) and at van der Waals contact with the phytol chain of Chl_{D1} (green, shown in stick presentation); electron density (blue) contoured at 1.2 σ level. C) View of the full Q_A molecule (magenta) with its head group bound to subunit D2 (orange) and the isoprenoid chain forming part of the binding pocket of Chl_{D1} (green). Parts of other proteins in the vicinity are shown in yellow (D1), orange (D2) and grey (PsbT).

There are also several other cofactors in the vicinity of the head group of Q_A , among them the lipid MGDG11, bicarbonate ion, non-haem Fe^{2+} cation and pheophytin Phe_{D1} . The head group of MGDG11 is at the shortest distance of 6.4 Å from the head group of Q_A , but they do not interact directly as they are separated by the phenyl group of conserved D1-Phe261. Bicarbonate ion and non-haem iron are 6.5-6.8 Å apart from Q_A and the latter is pierced by the pseudo C_2 (Fe^{2+}) axis [224]. The body of Phe_{D1} is screened from the Q_A tail by D2-Leu209 and D2-Ile213 residues (the shortest $Phe_{D1} \cdots Q_A$ distance is 4 Å) and is coupled via D2-Trp253 to quinone's head group (the shortest distances $Q_A \cdots D2-Trp253 \cdots Phe_{D1}$ are 3.4 Å and 3.3 Å, respectively).

3.2.2.2 Plastoquinone Q_B

In symmetry related position the second plastoquinone Q_B is found. The Q_B -binding site is formed exclusively by conserved residues from subunit D1: Met214, His215, Leu218, Val219, Tyr246, Ala251, His252, Phe255, Ser264, Phe265 and Leu271. Q_B is stabilized by two (three) hydrogen bonds (Fig. 38): D1-His215ND1 \cdots O1- Q_B (2.78 Å) and D1-Ser264OG \cdots O2- Q_B (2.85 Å), both residues are conserved, the latter bond might be replaced by D1-Phe265N \cdots O2- Q_B (2.84 Å).

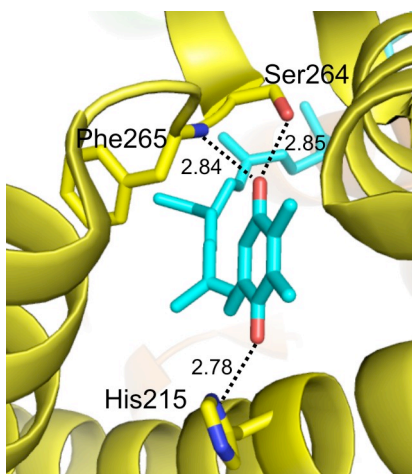


Figure 38. Hydrogen bonds between Q_B and the protein, all shown amino acids from subunit D1, distances are in Å.

The isoprenoid tail of Q_B , comprising seven of the nine expected isoprenoid units, is located in the novel plastoquinone-plastoquinol exchange channel II (Figs. 27 and 39), *vide infra*. The head groups of Q_B and Q_A are almost equidistant from the non-haem iron and

bicarbonate ion (Fig. 17). The plane of Pheo_{D2} is slightly tilted with regard to the Q_B tail and is in direct van der Waals contact with it (the shortest distance is 4.13 Å).

The binding pocket for Q_B is formed by a loop of subunit D1 that is close to lipids SQDG4, MGDG18 and PG22 (Fig. 36 and section 3.2.1.4). Although none of the lipids forms direct contacts with the head group of Q_B, the presence or absence of the lipids could indirectly tune the redox potential of Q_B [209].

Since plastoquinone Q_B must take up two electrons and two protons to be released into the plastoquinone pool in the thylakoid membrane, a constant supply of protons from the cytoplasmic side is required. The electron transfer occurs in two steps: the plastosemiquinone Q_B^{•-} is formed within $\sim 10^{-4}$ sec after a flash that produces a photon, characterized by high affinity to the Q_B-binding site, with further acceptance of the second electron after a second flash with somewhat slower kinetics [225]. The uptake of a proton occurs after or simultaneously with the acceptance of the first electron, and after the second flash (followed by the second electron transfer), the second protonation takes place [226]. The delivery of protons occurs through a hydrogen bond network, the shortest path from the cytoplasmic free-floating protons to the head group of Q_B being bridged by two amino acids, D1-His252 and D1-Ser264 (with hydrogen bonds His-ND \cdots OG-Ser, 2.90 Å and Ser-OG \cdots O2-Q_B, 2.85 Å respectively). This is in agreement with mutational experiments on D1-His252 [226, 227] that show the importance of this residue for proton transfer. The presence of the non-haem iron that is not involved in energy transfer [228-230] might play a role in tuning of the hydrogen-bond network near Q_B and could influence long range interactions as found for PBRC [231].

3.2.2.3 Plastoquinone Q_C

The electron density revealed the presence of a third and novel plastoquinone Q_C located in the PQ/PQH₂ exchange cavity (Figs. 27 and 39), in agreement with a stoichiometry of at least 2.5 PQ/35 Chl per PSII monomer of crystalline PSII from *T. elongatus* [61, 232] and consistent with other experiments that showed the presence of an additional exchangeable quinone molecule besides Q_B [233, 234]. Only five of the nine expected isoprenoid units could be modelled, indicating partial disorder and/or mobility of Q_C. This is supported by the finding that Q_C forms no hydrogen bonds stabilizing its position and has no well-defined binding pocket. This could indicate that the actual binding site Q_C is either in some other position (presumably close to the found location of Q_C, *e. g.* D1-Trp278 might serve as anchor which is 5 Å away and closer to *cyt b-559*) or a specific binding site might be absent at all. Q_C

resides in channel I with an exit portal between PsbJ and *cyt b-559* (Figs. 27, 39) and forms van der Waals contacts with carotenoid Car_{D2}, fatty acids SQDG4, MDGD7, the isoprenoid chain of Q_B and the phytol chain of Chl_{D2}, and with hydrophobic residues of subunits PsbJ and PsbF. Its head group is ~17 Å away from the head group of Q_B and ~15 Å from the haem of *cyt b-559* (edge-to-edge distances), in agreement with the proposal of a PQ-site near *cyt b-559* [235, 236].

3.2.2.4 The plastoquinone / plastoquinol exchange cavity

There is a large internal cavity with approximate dimensions of $36 \times 21 \times 25$ Å³ found in PSII and designed for plastoquinone/plastoquinol exchange. The cavity is defined by TMHs of PsbJ, PsbK, *cyt b-559*, TMHs **d** and **e** of D1, **a** of D2 and **f** of CP43. The cavity is lined with hydrophobic amino acids and filled with phytol chains of chlorophylls P_{D2}, Chl_{D2}, Chl37, Chl44, Chl46 and Pheo_{D2}, and the acyl chains of PG3, PG22, SQDG4, DGDG5, DGDG6, MGDG7, MGDG18, MGDG19. Moreover, the haem group of *cyt b-559* and the ionon rings of Car_{D2}, Car12, Car15 are exposed to the cavity.

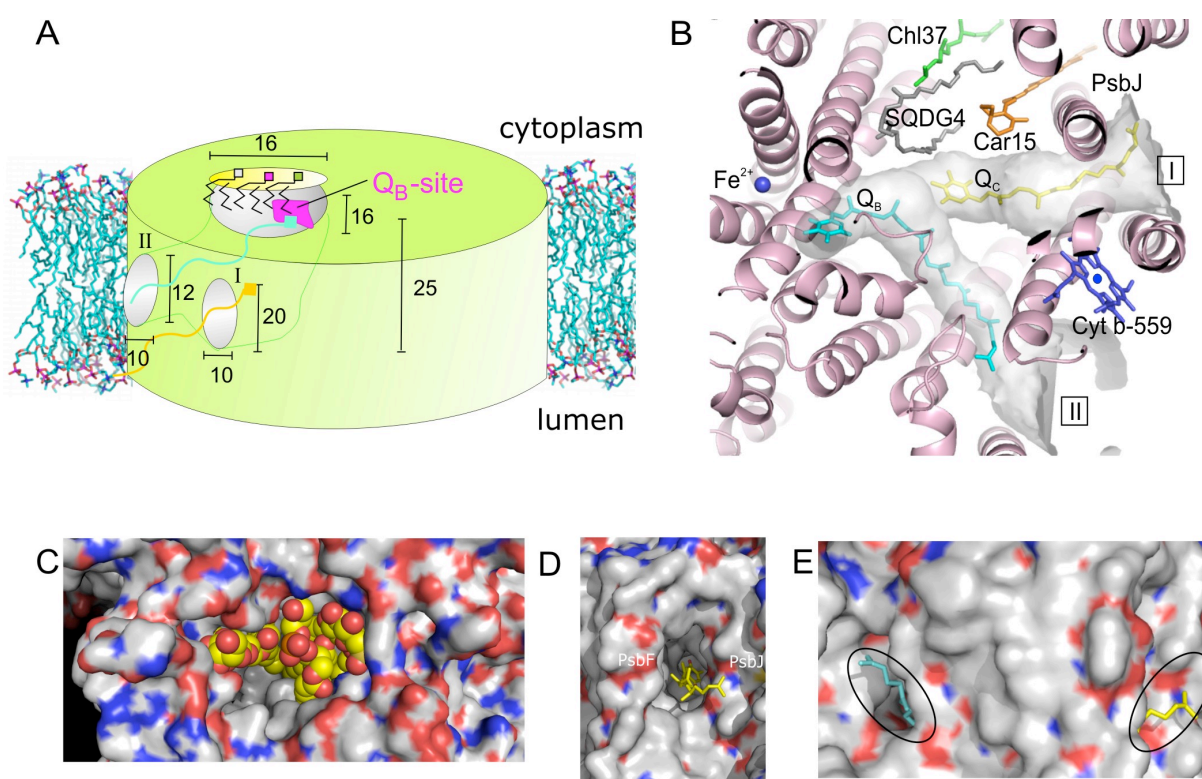


Figure 39. The quinone exchange cavity in PSII. (A) Schematic view of the PQ/PQH₂ exchange cavity and the two entry and exit portals connecting the Q_B site to the PQ pool in the thylakoid membrane. Approximate dimensions are given in Å; Q_B and Q_C are coloured cyan and yellow, respectively, the Q_B site is highlighted in

magenta and the three lipids forming the cork (the head groups of PG22, SQDG4 and MGDG18 are shown as red, green and white squares) nearly closing the cavity toward the cytoplasm are indicated. (B) Calculated channels (I and II, grey) for PQ/PQH₂ transfer between the PQ pool and the Q_B site, viewed from the cytoplasmic side. Shown are plastoquinones Q_B (cyan) and Q_C (yellow), non-haem Fe²⁺ (blue sphere), Car15 (orange), Chl37 (green), SQDG4 (grey), *cyt b-559* haem (dark blue) and the surrounding proteins (pink). Car_{D2}, Chl_{D2} and MGDG7 are not shown. (C) The lipid “cork” blocking PQH₂ release to the cytoplasm; lipids are shown as yellow (carbon) and red (oxygen) spheres. (D) View onto channel I, protein is shown as surface, Q_C as yellow stick model. (E) View onto channels I and II, same as panel (D), Q_B is in cyan, Q_C is in yellow.

The cavity shows three distinct openings, the largest one with approximate dimensions $16 \times 16 \text{ \AA}^2$ [41] leading to the cytoplasm and two smaller openings, named channel I and II, connecting the Q_B-binding site to the plastoquinone pool in the membrane phase. The large opening is nearly sealed with lipids PG3, SQDG4, MGDG18 and PG22 (with additional space for one or two lipids, Fig. 39), thereby preventing unfavourable release of PQH₂ to the cytoplasm. It was suggested [237] that this opening might be the anchor place for phycobilisomes *in vivo*. Channel I opens into the exit portal with dimensions $10 \times 20 \text{ \AA}^2$ between TMHs of PSbJ and *cyt b-559* [41], ca. 30 Å away from the Q_B-binding site, while the exit portal of channel II with dimensions $12 \times 10 \text{ \AA}^2$ is located between TMHs of PsbF and a of D2, ca. 23 Å away from the Q_B-binding site.

Such arrangement of channels is well suited for the fast exchange of reduced PQH₂ with fresh PQ from the PQ-pool in the thylakoid membrane, because for rapid turnover of water at the Mn₄Ca cluster (see section 3.2.3) of PSII it is necessary that the final electron acceptor plastoquinone at the Q_B site is always available in sufficient amounts. After charge separation has occurred, an efficient oxidation of the transiently formed primary semiquinone Q_A⁻ is especially important as accumulation of it could lead to charge recombination reactions and finally formation of deleterious triplet states at the primary donor Chls (³P680). In contrast to several other quinone binding proteins, the quinone binding sites in PSII are not located towards the membrane exposed surface of the complex but they are rather buried deep within the D1/D2 heterodimer.

3.2.2.5 Mechanisms for plastoquinone / plastoquinol exchange

The novel plastoquinone Q_C found in our structural model and the arrangement of PQ molecules relative to the entry/exit portals suggests three possible mechanisms for PQ/PQH₂ exchange between the Q_B-site and the PQ-pool:

(1) Alternating (Fig. 40) - Entry and exit of PQ and PQH₂ both proceed through channels I and II in an alternating way. After reduction and double protonation of Q_B, PQH₂ leaves PSII through channel II, and Q_C in channel I moves and binds to the Q_B-site with its isoprenoid tail still located in channel I. Simultaneously another PQ from the PQ-pool enters the transiently empty channel II. After reduction/protonation, PQH₂ leaves the Q_B-site now through channel I, and PQ from the PQ-pool moves along channel II and binds to the Q_B-site for another cycle.

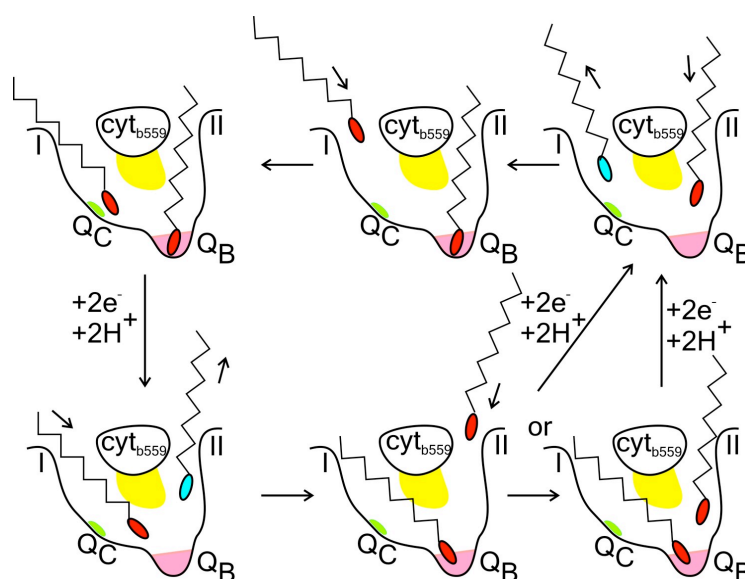


Figure 40. The alternating mechanism. Channels I and II open towards the PQ pool. PQ is shown with a red and PQH₂ with a blue head group. The Q_B site is highlighted pink, the Q_C “site” in green and labelled; the yellow patch indicates a hydrophobic region formed by the fatty acids of MGDG7, MGDG18 and the phytol chain of Chl_{D2}. Small arrows symbolize movements of PQ molecules.

(2) Wriggling (Fig. 41) – Entry of PQ occurs exclusively through channel I, and PQH₂ exits through channel II. After reduction/protonation, PQH₂ leaves the Q_B-site through channel II, and Q_C enters the Q_B-site from channel I. After or simultaneously with binding to the Q_B-site, the isoprenoid tail wriggles around the hydrophobic tails of Chl_{D2}, MGDG7 and MGDG18, which are located between the two channels (yellow patches in Figs. 40-42). The isoprenoid tail finally points into the empty channel II, and another PQ from the PQ-pool enters the Q_C-site through channel I.

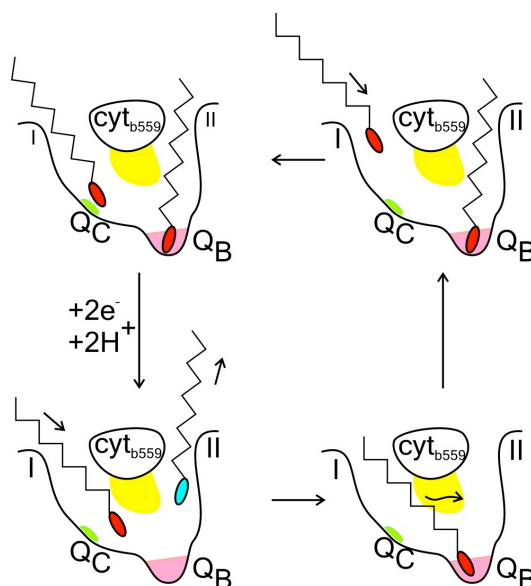


Figure 41. Wiggling mechanism.

(3) Single channel - Entry and exit proceed only through channel II, channel I being not involved in PQ/PQH₂ exchange. After reduction/protonation, PQH₂ leaves the Q_B-site through channel II, and PQ from the pool enters the empty channel II and binds to the Q_B-site for a next cycle. PQ in the Q_C-site remains at this position and does not participate in PQ/PQH₂ exchange.

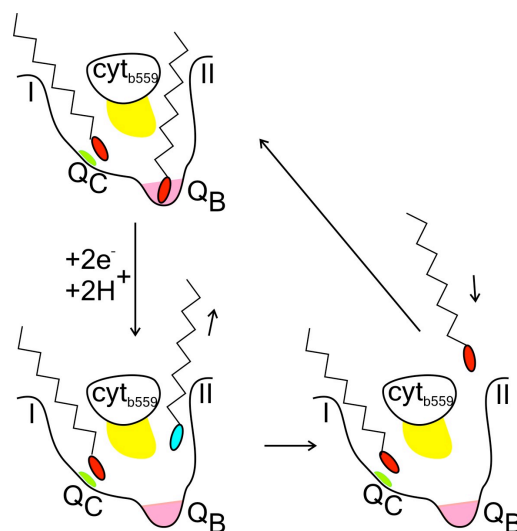


Figure 42. Single channel mechanism.

In mechanisms (1) and (2), the second mobile PQ molecule (Q_C) is replacing Q_B for rapid turnover to avoid delays in electron transfer. Mechanism (3) provides no actual

replacement of Q_C , but the latter might have other as yet unknown functions in secondary electron transfer or, in cooperation with *cyt b-559*, in the regulation of PSII function. All three mechanisms lead to a decrease of deleterious back-reactions even under low PQ concentrations in the PQ-pool and might be utilized under different ambient conditions.

Based on electron microscopy data for PSII from *Spinacia oleracea* [238, 239], the structural model of the LHCII-PSII supercomplex [240] and on the high degree of identity between cyanobacterial and plant PSII, it is conceivable that a similar quinone/quinol exchange cavity does exist in plant PSII.

An analysis of quinone molecules in photosynthetic complexes reveals a general and interesting feature – all quinones are accompanied by lipid molecules, suggesting that lipids are necessary for quinone/quinol exchange (*e.g.* the largest lipid cluster in PSII, Fig. 30, facilitating PQ exchange by providing a hydrophobic environment). Indeed, the diffusion coefficient of quinones in protein-free liposomes is two order higher than in thylakoids [241]. This dramatic difference is caused by significant protein content in the thylakoid membranes, up to 70% [242]. Since proteins are obstacles for the free diffusion of quinone molecules, their size and shape are crucial for the diffusion rate of quinones [243]. It was shown [242] that the travel time of quinone PQ from PSII to the neighboring *cyt b6f* complex increases from 10 μ s in obstacle-free membrane to 8ms in the thylakoide membrane.

Monte-Carlo simulations of the diffusion of PQ within the thylakoid membrane with random protein arrangement [243] indicated that quinone movements are restricted to small lipid areas within the membrane, termed microdomains [244-246], with maximum length of 200 Å. Other means to diminish the hindered diffusion caused by protein crowding would be the formation of supercomplexes, as it is easier for quinone molecules to diffuse between few bulky obstacles than between many small ones [247]. A structurally ordered arrangement of proteins might also favour quinone diffusion [248]. Indeed, there is some evidence of ordered arrays of protein complexes in the thylakoid membrane under stress as well as under normal conditions as shown for bacteria [249, 250] and plants [251, 252]. As proposed [247], such ordered arrangement of PSII complexes might facilitate quinone/quinol exchange as the access to the channels leading to Q_B -binding sites would be less hindered.